HYDROGEN PRODUCTION USING HIGH-TEMPERATURE STEAM ELECTROLYSIS SUPPORTED BY ADVANCED GAS REACTORS WITH SUPERCRITICAL CO_2 CYCLES

FISSION REACTORS

KEYWORDS: *high-temperature steam electrolysis, advanced gas reactor, supercritical CO_2 cycle*

BILGE YILDIZ,* KATHERINE J. HOHNHOLT, and MUJID S. KAZIMI
Massachusetts Institute of Technology, Center for Advanced Nuclear Energy Systems
Cambridge, Massachusetts 02139-4307

Received April 26, 2005
Accepted for Publication September 28, 2005

Hydrogen production using high-temperature steam electrolysis (HTSE) supported by a supercritical CO_2 (SCO_2) recompression Brayton cycle that is directly coupled to an advanced gas-cooled reactor (AGR) is proposed in this paper. The system features and efficiency are analyzed in a parametric fashion. The analysis includes the influence of the major components' performance and the component integration in a proposed plant layout. The configuration, HTSE-SCO_2-AGR, with thermal recuperation from the product gas streams and an intermediate heat exchanger between the turbine exit and the feedwater stream is found to offer excellent thermal efficiency, operational flexibility, and expected cost. The HTSE average process temperature is 900°C, and the hydrogen pipeline delivery pressure is assumed to be 7 MPa for the evaluation of the plant performance. The reactor exit temperature and the SCO_2 cycle turbine inlet temperature are the same as those for the SCO_2 recompression cycle design: 550 to 700°C. The 900°C at the HTSE unit, which is higher than the reactor exit temperature, is achieved with recuperative and electrical heating. HTSE is assumed to operate within 80 to 90% voltage efficiency at 1 atm to 7 MPa of pressure. A parametric analysis of these operating conditions shows that the system can achieve 38.6 to 48.2% low heating value of net hydrogen production energy efficiency. The extensive experience from commercial AGRs, the compactness of the SCO_2 power conversion system, and the progress in the electrolysis cell materials field can help the economical development of a future recuperative HTSE-SCO_2-AGR. The major research and development needs for this plant concept are materials processing for the durability and efficiency of the HTSE system, the design update of the AGR with advanced materials to resist high-pressure CO_2 coolant, thermal hydraulics of CO_2 at supercritical pressures, and detailed component design for system integration.

I. INTRODUCTION

The fast-growing worldwide demand for energy combined with increasing greenhouse gas CO_2 emissions and diminishing total fossil fuel reserves has made it critical to increase the efficiency of total fuel utilization and to expand alternative sources of energy. One of the more promising alternative technologies for the transportation energy sector is hydrogen-fueled fuel cells to reduce CO_2 emissions, to end the dependence on petroleum, and to prepare for the time at which oil reserves become depleted. Nuclear energy is a candidate to supply the energy needed for extracting the hydrogen from water or other molecules while avoiding concerns related to CO_2 emissions.

In previous work,[1–3] we provided a brief assessment of energy efficiency and preliminary economics of alternative nuclear hydrogen production technologies. One of our results was that an integrated system of a high-temperature steam electrolysis (HTSE) unit supported by a supercritical CO_2 (SCO_2) power conversion system that is directly coupled to an advanced gas-cooled reactor

*E-mail: byildiz@anl.gov

(AGR) can be more energy efficient and more readily feasible than other alternative technologies for nuclear hydrogen production (such as high-temperature sulfur processes), especially over an intermediate temperature range of operation (650 to 750°C). The preliminary analysis[1,2] did not address the opportunities to improve the system performance. This paper presents an investigation of some design aspects of this system, the HTSE-SCO_2-AGR, and the technical issues for its development.

I.A. Nuclear Hydrogen Production Processes

Several studies evaluated the candidate technologies for nuclear energy–supported hydrogen production.[1–4] Currently, the leading alternatives for nuclear hydrogen production are the HTSE (Refs. 5, 6, and 7), the Westinghouse hybrid sulfur process[8] (WSP), and the sulfur-iodine (SI) thermochemical process.[9] Other processes have also been suggested but are less developed. The main three technologies have been tested at lab scale but need further development and demonstration for proof of system integration feasibility, operability, and economics. In addition to the HTSE, WSP, and SI processes, the Cu-Cl and UT-3 thermoelectrochemical processes are also investigated by several groups for hydrogen production supported by nuclear energy, as summarized by Yildiz and Kazimi.[1–3] The Cu-Cl and the UT-3 processes have been proposed to achieve hydrogen production efficiency of ~33 to 37% at 500°C and 34% at 740°C, respectively. However, although the original UT-3 cycle has been demonstrated, both of these processes are less developed than the HTSE, WSP, and SI processes.

An efficiency estimate of the nuclear hydrogen production technologies has been made based on an integrated system that couples the hydrogen production process to the nuclear reactor in a simple layout with no thermal recuperation at the interface.[1,2] Figures 1 and 2 show, respectively, the schematics for the thermochemical processes that do not require electricity input and the electrothermochemical processes that require electricity input in addition to thermal energy input. Both the thermochemical and thermoelectrochemical processes can involve thermal recuperation within the stages of the decomposition process, however, not necessarily in an optimized way as of now. Figure 3 indicates the efficiency advantage of high-temperature steam electrolytic hydrogen production coupled to intermediate/high-temperature gas-cooled reactors, especially over intermediate temperature ranges.

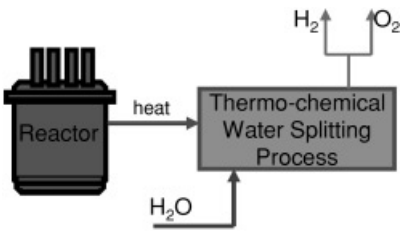

Fig. 1. Schematics for the simple coupling of the thermochemical water-splitting process and nuclear reactor for hydrogen production.

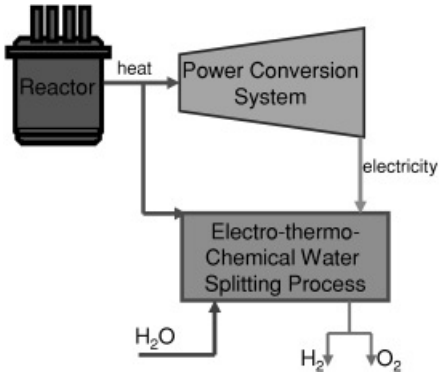

Fig. 2. Schematics for the simple coupling of electrothermochemical water-splitting process, nuclear reactor, and power conversion system for hydrogen production.

I.B. Objective and Scope of This Work

As seen in Fig. 3, base case HTSE-SCO_2-AGR technology can promise higher efficiency, especially at intermediate to high temperatures. This advantage is primarily due to the higher efficiency of the SCO_2 recompression Brayton cycle that is designed to operate well at intermediate temperatures. Thus, our objective in this work is to define configurations for system components and their operational conditions to further improve the overall energy efficiency of the integrated system, HTSE-SCO_2-AGR. Consequently, the improved design performance of nuclear hydrogen production technologies (such as the HTSE-SCO_2-AGR) can be compared to nonnuclear alternatives for hydrogen production on a more consistent and sound basis.

Based on the analysis in this work, the HTSE-SCO_2-AGR can be founded on the development of four major technologies:

1. the HTSE H_2 production units composed of solid oxide electrolysis cells (SOEC)
2. the efficient and compact SCO_2 recompression Brayton cycle power conversion system with a maximum temperature range of 550 to 700°C and pressure of 22 MPa
3. updated AGR units operating at 20 MPa, based on those that have been commercially operating in the United Kingdom at 4 MPa of reactor pressure since 1976

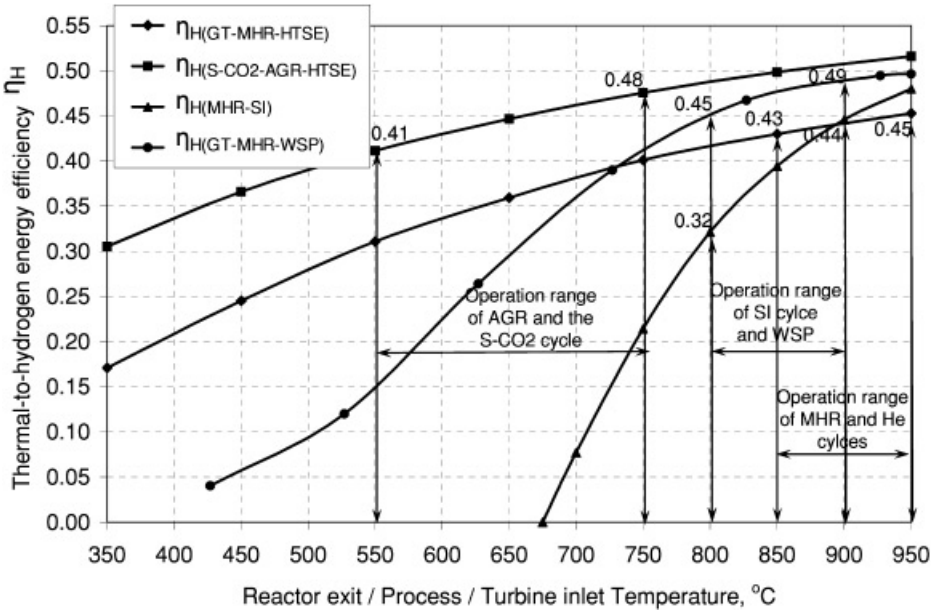

Fig. 3. Thermal-to-hydrogen energy efficiency (using the LHV of hydrogen) of nuclear H_2 production technologies.[2]

4. compact and highly effective heat exchangers that can operate at high pressures and temperatures, such as the printed circuit–type heat exchangers (PCHE) by Heatric.

In this paper, we assess the thermodynamics of an integrated HTSE-SCO_2-AGR system and identify opportunities for improved design layout and operating conditions for better thermal-to-hydrogen efficiency. In doing so, we consider the key features of the necessary technological developments for this design: the performance of candidate HTSE materials, the operating conditions of the SCO_2 recompression Brayton cycle, the material restrictions under high temperature and pressure CO_2 environment for an updated AGR, and the effectiveness of heat exchangers that can be included into this system.

The paper is structured as follows. Section II explains the characteristics of the HTSE systems and provides the basis of some HTSE performance-related assumptions used in the plant thermodynamics analysis. Section III gives a summary of the SCO_2 system based on the design by Dostal et al.,[10] describes the AGR and explains the necessary design upgrades for a new supercritical pressure AGR concept to be ready for hydrogen production, and summarizes the effect of CO_2 corrosion-related issues on the design of the integrated nuclear hydrogen production system. Section IV presents the energy efficiency analysis and improved plant configuration for the HTSE-SCO_2-AGR. Section V provides the concluding remarks of our work and the future research needs of the design presented in this paper.

II. HIGH-TEMPERATURE ELECTROLYSIS

The HTSE process uses thermal energy and electricity to split steam into hydrogen and oxygen in a solid state electrochemical device. The electrochemical device for the HTSE process can be called an SOEC. To a first approximation, the electrochemistry of SOEC is the reverse of that of a solid oxide fuel cell (SOFC). The transport process within an SOEC is schematically shown in Fig. 4. The high-temperature operation for steam electrolysis is favorable in terms of both the thermodynamics of the process and the kinetics related to the materials of SOEC.

For the endothermic reaction $H_2O_{(g)} \rightarrow H_{2(g)} + \frac{1}{2} O_{2(g)}$ that can take place in a control volume, such as the SOEC system, the change in Gibbs free energy of the reaction ΔG, that is the difference between the chemical potential of products and reactants, is given as

$$\Delta G = \Delta G_0 + RT \ln \frac{P_{H_2} P_{O_2}^{1/2}}{P_{H_2O}} \quad . \tag{1}$$

As the temperature increases, ΔG_0 for electrolysis decreases. For an electrolytic cell, the minimum reversible electrical work necessary for the process is equivalent to the difference between the electrochemical potential of products and reactants, which is ΔG. Hence, for a reversible system,

$$W_{min} = -\Delta G \quad . \tag{2}$$

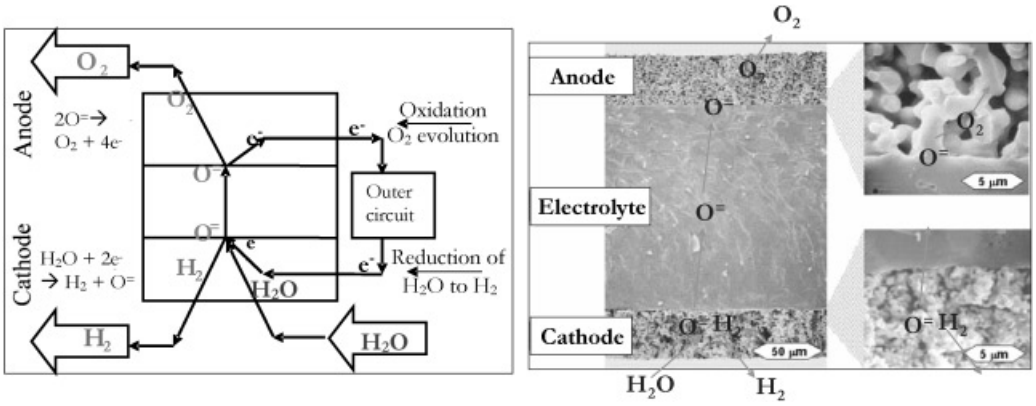

Fig. 4. Transport process within an SOEC.[a]

Finally, the reversible voltage E_r of the electrolysis of any reactant gas is

$$E_r = \frac{-\Delta G}{n_e \cdot \Im} \quad , \tag{3}$$

where n_e is the number of electrons (two for electrolysis of water) and $\Im$ is the Faraday constant (96 485 C/mol). Equation (3) allows one to express the reversible cell voltage in terms of the Nernst relation:

$$E_r = E_0 - \frac{RT}{2\Im} \ln \frac{P_{H_2} P_{O_2}^{1/2}}{P_{H_2O}} \quad . \tag{4}$$

However, in actual operation, electrochemical systems encounter irreversibilities that lead to energy losses. In an electrolytic cell, these irreversibilities are due to three main mechanisms: The first is the activation a of reactions for the evolution of H_2 and O_2 at the surface of the electrodes, the second is the mass transfer c of species to and within the porous electrodes, and the third is the ohmic resistance Ω against the diffusion of oxygen ions and electrons. In electrolysis, these irreversibilities translate to additional electrical potential required for overcoming each of the mechanisms that contribute to the irreversibility. The additional electrical potential for electrolysis is called the overpotential. $\eta = |E - E_r|$ represents the overpotential energy loss. Its components are η_a, η_c, and η_Ω, respectively. Hence, the actual voltage to be applied on the electrolytic cell (SOEC in this case) is expressed as

$$E_R = E_0 - \frac{RT}{2\Im} \ln \frac{P_{H_2} P_{O_2}^{1/2}}{P_{H_2O}} - (\eta_a + \eta_c + \eta_\Omega) \quad ,$$

where $E_0 < 0$. (5)

The potential that is required for electrolysis depends also on the hydrogen production rate per unit area that is directly proportional to the current density in the electrolytic cell. Typical behavior of the required cell voltage and the associated power density applied on unit cell area as a function of current density is shown in Fig. 5. Contrary to SOFCs, there is no optimal power density. The SOEC power density increases as the H_2 production rate (i.e., the current density) increases. At each current density, the efficiency of an SOEC can be represented by the voltage efficiency

$$\eta = \frac{|E_r|}{|E|} \quad . \tag{6}$$

At a given operating temperature, the SOEC materials must be chosen to minimize the overall

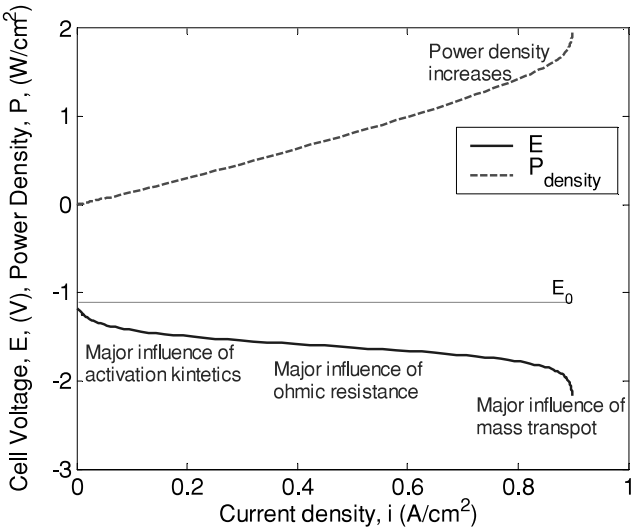

Fig. 5. Dependence of SOEC cell voltage and power density on current density (example plot for theoretical modeling of an LSM-YSZ-Ni/YSZ system at 700°C).

[a]The SEM micrograph of an electrolyte-supported SOFC is taken from Ref. 13 and is modified to show the SOEC representation.

overpotential while maximizing the achievable current density (the production rate). This objective is equivalent to minimizing the irreversibilities.

The SOECs can operate using electroceramic materials for the electrolyte and electrodes similar to those developed for solid oxide fuel cells. The most commonly established materials for the SOFCs have also been experimented in the SOEC mode of operation for hydrogen production. These are strontium-doped lanthanum manganite (LSM) as the anode, yittria-stabilized zirconia (YSZ) as the electrolyte, and Ni-YSZ composite cermet as the cathode.[5–7] An analytical comparison of the electrochemical performance of several SOFC materials in the SOEC mode of operation is presented by Yildiz et al.[12] Better-performing material candidates for oxygen electrodes of SOECs have been developed and presented by Meyers et al.,[13] and improvement for hydrogen electrode in SOEC operation is ongoing.

For the purposes of the analysis of an integrated H_2 production plant in this work, we assume that the overpotential losses can amount to a certain percentage of the reversible cell voltage, rather than referring to specific materials system. A voltage efficiency of 90% is typical for the SOFCs as a goal in the future at relatively high current density. Therefore, conservatively, we assume that the overpotentials in the operation of SEOC units can amount to 10 to 20% of the reversible cell voltage. This range is used in the calculations for estimating the thermal efficiency of the integrated system in Sec. IV.

III. SCO_2 ADVANCED GAS-COOLED REACTOR AND POWER CONVERSION SYSTEM

III.A. SCO_2 Turbine Power Conversion System

Dostal et al.[10] presented a systematic optimization of SCO_2 Brayton power cycles for application under practical constraints to advanced nuclear reactors. This study shows that the recompression cycle excels with respect to simplicity, compactness, cost, and thermal efficiency. The layout of the SCO_2 recompression Brayton cycle is schematically shown in Fig. 6.

The thermodynamic optimization of the system included the sizing and the effectiveness of the individual components. For the basic design, a conservative temperature for the turbine inlet was selected as 550°C, and the compressor outlet pressure was set at 20 MPa. For these operating conditions the direct cycle can achieve 45.3 to 46.6% of thermal efficiency. The cost of the power plant was estimated to be ~18% less expensive than one using a conventional Rankine steam cycle. The capital cost of the basic design is about equal to one using a helium Brayton cycle, but the SCO_2 cycle operates at significantly lower temperatures. The reactor operating experience with CO_2 as coolant, for instance British AGRs, is up to 650°C. The turbine inlet temperature of 650°C

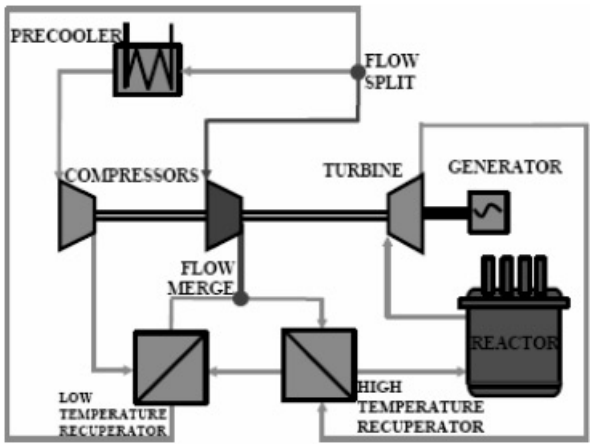

Fig. 6. Layout for the SCO_2 recompression Brayton cycle.[10]

was evaluated as an advanced design alternative for the SCO_2 recompression Brayton cycle. The thermal efficiency of the advanced design would be close to 49.5 to 50.6%, and the reactor system with the direct SCO_2 cycle is then ~24% less expensive than the steam indirect cycle and 7% less expensive than a helium direct Brayton cycle. It is expected in the future that high-temperature materials will become available, and consequently, a high-performance design with turbine inlet temperatures of 700°C would be possible. This high-performance design achieves a thermal efficiency approaching 53%, which can yield additional cost savings.

The operating conditions and the effect of turbomachinery efficiency on the thermal gross and net efficiency of the system are presented in Table I.

The main advantage of the SCO_2 turbine power conversion system over the He turbine power conversion system is its capability to achieve comparable or higher energy efficiency at significantly lower temperatures (550 versus 850°C) with a more compact and simple system layout. This advantage can play an important role in favor of using this system for Generation-IV reactors. Much detail can be found in Ref. 10 about the design development for the SCO_2 recompression Brayton cycle.

The SCO_2 cycle can be supported by any type of reactor that has a reactor exit temperature of above 550°C in either a direct or indirect way. We propose the direct coupling of the SCO_2 cycle to an updated design AGR, for its advantageous implications in terms of energy and cost savings, for a nuclear hydrogen production plant. We adopt the design alternatives and operating conditions presented in Table I for the SCO_2 system in calculating the performance of the new HTSE-SCO_2-AGR system.

III.B. Advanced Gas-Cooled Reactor

The AGRs have been commercialized in the United Kingdom since 1976. This section first briefly describes

TABLE I

Operating Conditions of the Selected Designs for the Recompression SCO_2 Recompression Brayton Cycle*

Turbomachinery Design	Basic Design		Advanced Design		High-Performance Design	
	Con.[a]	B.E.[b]	Con.	B.E.	Con.	B.E.
Cycle thermal power [MW(thermal)]	600	600	600	600	600	600
Thermal efficiency (%)	45.27	46.61	49.54	50.58	51.27	52.15
Net efficiency (%)	41.00	42.40	45.24	46.35	46.96	47.96
Net electric power [MW(electric)]	246	254	272	278	282	288
Compressor outlet pressure (MPa)	20	20	20	20	20	20
Pressure ratio	2.6	2.6	2.6	2.6	2.6	2.6
Primary system pressure drop (kPa)	130	130	130	130	130	130
Turbine inlet temperature (°C)	550	550	650	650	750	750
Compressor inlet temperature (°C)	32	32	32	32	32	32
Cooling water inlet temperature (°C)	27	27	27	27	27	27
Mass flow rate (kg/s)	3176	3246	2990	3027	2839	2877
Recompressed fraction	0.4	0.41	0.41	0.41	0.39	0.41
Total heat exchanger volume (m^3)	120	120	120	120	120	120
Turbine efficiency (%)	90.0	92.9	90.0	92.9	90.0	92.9
Main compressor efficiency (%)	89.0	92.9	89.0	92.9	89.0	92.9
Recompressed compressor efficiency (%)	89.0	93.0	89.0	93.0	89.0	93.0
Generator efficiency (%)	98.0	98.0	98.0	98.0	98.0	98.0
Mechanical losses (%)	1	1	1	1	1	1
Parasitic losses (%)	2	2	2	2	2	2
Switch yard losses (%)	0.5	0.5	0.5	0.5	0.5	0.5

*Adapted from Ref. 10.
[a]Conservative turbomachinery performance.
[b]Best-estimate turbomachinery performance.

the features of the commercial AGR, then discusses the design update that is proposed for AGR to support H_2 production by steam electrolysis.

III.B.1. Commercial AGR

The AGR was a direct development from the earlier gas-cooled MAGNOX reactors. The AGR units are of 660 MW(electric) capacity. The AGR fuel is enriched uranium oxide contained within stainless steel cans that allow a significant increase in operating temperature compared to that of previous MAGNOX-type reactors. The moderator is graphite as in the MAGNOX design. The reactor coolant is CO_2 at a system pressure of 4.2 MPa and a reactor exit temperature of 645°C. The core is enclosed within a prestressed concrete reactor vessel (PCRV) that has safety advantages. The vessel is made gas tight by a thin mild steel liner that is protected from the high gas coolant temperatures by foil and blanket insulation attached to its inner surface.

The AGR fuel pins are ~1 m long and are arranged in a 36-pin cluster within graphite fuel sleeves making up a fuel element. Eight of these elements are stacked together vertically in each fuel channel. This arrangement permits on-load refueling by allowing one pile cap standpipe to be provided per channel. The reactor is indirectly coupled to a Rankine cycle for electricity production. The steam generators, which are of once-through design, are located inside the pressure vessel. Figure 7 represents the schematics of the plant layout for a commercial AGR design. Table II summarizes the main design parameters of the AGR, based on the reference plant of Hinkley Point B.[15]

With the prototype plants, problems have been encountered during the construction, testing, and power-raising phases. However, engineering and operational solutions have been found for the majority of the problems. For instance, the higher gas temperatures and pressures, combined with higher power densities in the AGR, produced a more aggressive environment for all materials in the circuit than that in a MAGNOX reactor. The two conflicting materials issues due to the operating conditions were graphite corrosion and carbon deposition on the fuel. By operational experience, a coolant composition has been determined as a compromise between the requirement to inhibit these tendencies, based upon levels of CO, CH_4, and H_2O in the CO_2 coolant gas.[15–17] Extensive experience and data have been gained on the issues of materials in a CO_2 environment through the operation of AGRs. This experience can help the design

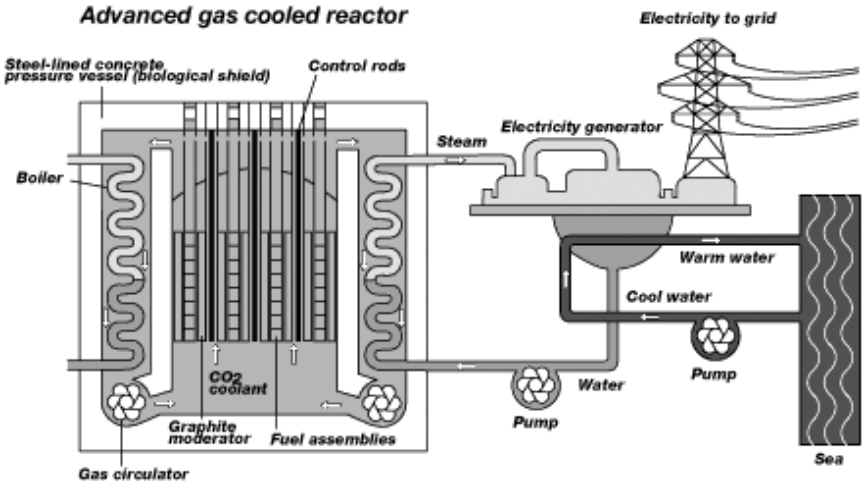

Fig. 7. Advanced gas-cooled reactor, commercial design schematics.[14]

TABLE II

Hinkley Point B (AGR) Design Parameters*

Electrical output (MW)	660
Overall thermal efficiency (%)	41.6
Reactor thermal power (MW)	1493
Mean channel gas temperature, inlet (°C)	319
Mean channel gas temperature, outlet (°C)	645
Coolant pressure (bar)	42.4
Core diameter (m)	11
Core height (m)	9.8
Mean fuel element rating [MW(electric/tonne)]	5.14
Mean fuel element length (mm)	1039
Mean pin diameter (mm)	14.5
Enrichment, wt% ^{235}U	2.55
Turbine stop valve pressure (bar)	160
Turbine stop value temperature (°C)	538
Turbine stop value reheat pressure (bar)	39
Turbine stop value reheat temperature (°C)	538
Turbine stop value feedwater temperature (°C)	156

*Adapted from Ref. 15.

of future AGRs to operate in a more efficient and cost-effective way.

III.B.2. Updated AGR Design Concept

Here, we explore a direct cycle AGR using an SCO_2 gas turbine for viability. This concept has also been studied in the past and has been proposed to be feasible.[15] Various cycles were studied in the 1970s (Ref. 15) that gave efficiencies mostly in the region 38 to 40% for a top gas temperature of 700°C (this estimate of efficiency is lower than the design in Ref. 10 can achieve). Nevertheless, the technology to develop an SCO_2 turbine directly coupled to a nuclear reactor was not present at that time, and this concept has not been brought to realization. With the progress in gas turbine technology that has taken place over time, such an integrated system can be more compact and cheaper than a steam cycle unit of similar output. For instance, the most costly component of the commercial AGR was the steam generator,[16] and this component would be eliminated by a direct-cycle supercritical pressure design. The most important change required in the operation of an AGR to allow the use of a direct-cycle SCO_2 recompression Brayton cycle would be the increased coolant pressure up to 20 MPa to match the turbine inlet design pressure of this cycle.

II.B.2.a. Reactor Pressure Vessel. The increased pressure requires design update, especially of the structural components such as the reactor pressure vessel and containment. The prestressed concrete pressure vessel of commercial AGRs may not safely withstand the 20 MPa of system pressure. One solution may be to make the walls of the pressure vessel much thicker. This can have high cost implications. Another approach may be the use of a prestressed cast iron pressure vessel (PCIV). This technology has been chosen by Massachusetts Institute of Technology as a prime candidate for application to a gas-cooled fast reactor (GFR) because of its high assurance against coolant leakage at a cost that is competitive with that of PCRVs or conventional forged steel vessels.[18] A PCIV is an assembly of cast iron blocks interlaced with tensioned cables around a welded steel liner as shown in Fig. 8. Leak tightness is provided by an inner liner. The segments can be easily transported to any place and have to be assembled and prestressed on-site. The multitendon arrangement excludes any possibility for a sudden burst as already proven by experiments. Large cracks cannot progress as the compressive stresses are superimposed with the tensile stresses due to internal

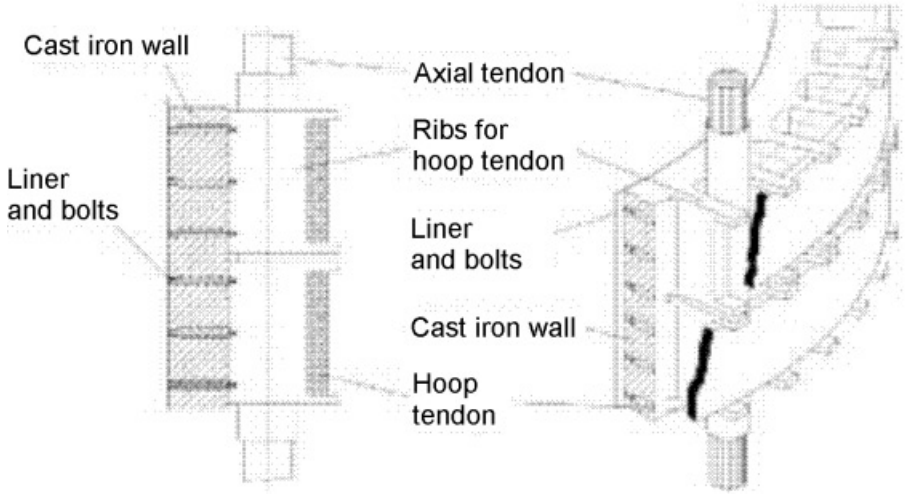

Fig. 8. Characteristic PCIV wall.[19]

pressure. Passive decay heat removal via the PCIV structure has also been tested and could be improved by integration of a passive vessel cooling system within the PCIV wall. This could also improve the heat transfer mechanism and open the potential for enlarging the power size of a modular high-temperature reactor or other types of modular reactors as well.[19]

II.B.2.b. Reactor Neutronics. The increased pressure of CO_2 is not expected to affect significantly the neutronics of the new supercritical pressure AGR concept. Since the moderator of AGR is graphite, the increase in the density of CO_2 at 20 MPa has negligible effect on the reactivity increase. A preliminary analysis of the reactivity feedback due to pressurization of a CO_2-cooled core (20 MPa) of GFR design indicated an insignificant increase in the reactivity due to coolant density. A similarly small effect is expected for the influence of high-pressure CO_2 on AGR net reactivity.

II.B.2.c. Reactor Thermal Hydraulics. Thermal hydraulics of the SCO_2 needs to be studied further for better understanding the change in the physical properties of the fluid and their implications to the heat transfer capability of CO_2. Enhanced heat transfer performance is expected at supercritical pressure due to the high heat capacity of CO_2 and its low viscosity. The core configuration may be redesigned to make the reactor core somewhat more compact by utilizing increased graphite and the improved thermal properties of the supercritical coolant, while still keeping the thermal neutron spectrum. The possibility for passive safety capability needs to be studied for this new AGR. A detailed design and heat transfer optimization are needed to maximize potential reactor-cooling system performance.

III.B.2.d. Materials. Durability of materials under supercritical pressure and an intermediate temperature CO_2 environment is essential for the success of both the SCO_2 power conversion system and the new AGR concept. There is extensive experience gained in AGR operations for inhibiting the reaction of CO_2 with structural materials, cladding, and graphite that causes material corrosion. This experience can guide the design update of the supercritical AGR concept with appropriate materials selection. However, most of the tests in this area for understanding the corrosion behavior in CO_2-based coolant and the AGR operations have been held at relatively low pressures. Theoretical modeling and tests on materials for corrosion under supercritical pressure CO_2 should be performed to validate the durability of the materials proposed for an updated design, with guidance from operational AGRs' experience. The materials-related issues that have been overcome in AGR operations are presented in more detail in Ref. 11.

IV. H_2 PRODUCTION PLANT: HTSE-SCO_2-AGR

A nuclear hydrogen production plant should be designed to recuperate as much heat from the product streams as feasible to improve the energy efficiency and the cost of production. The earlier analysis in Refs. 1 and 2 for the HTSE-SCO_2-AGR efficiency considered a simple plant layout as in Fig. 9. In such a plant configuration, thermal recuperation is not optimized. The efficiency recorded in Fig. 3 for the HTSE-SCO_2-AGR corresponds to the configuration as in Fig. 9, with irreversibilities in the HTSE unit equivalent to 10% of the ideal electrical energy needed for the electrolysis. Table III summarizes the thermal-to-hydrogen energy efficiency (using LHV of hydrogen) of this system with the simple base case design layout, using the turbine inlet conditions that match the SCO_2 cycle design options. There is significant margin for improving

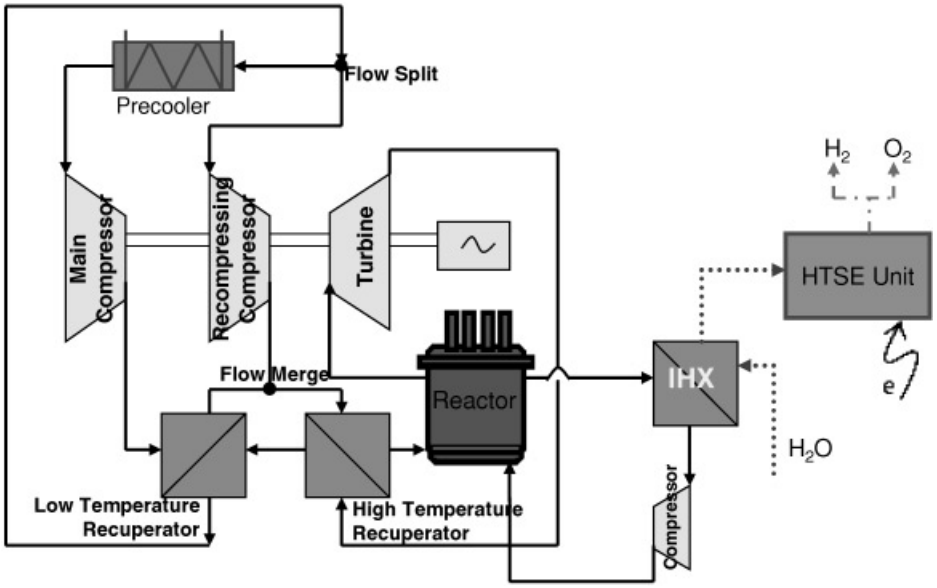

Fig. 9. Simple plat layout for HTSE-SCO_2-AGR.

TABLE III

Thermal-to-Hydrogen Energy Efficiency of a System as in Fig. 9 as a Function of Temperature, at 1 atm with No H_2-Compression

Turbine inlet/HTSE temperature (°C)	550	650	700
Process efficiency (LHV) (%)	41	45	46

the efficiency and the economics of hydrogen production from an HTSE-SCO_2-AGR plant with thermal recuperation from the product streams.

IV.A. Thermodynamics of H_2 Production Using Recuperative HTSE-SCO_2-AGR

The product gases from the HTSE are ideally pure hydrogen and oxygen. The product gases are produced at high temperatures due to the process operating conditions. Hence, the thermal energy content of the product streams can be utilized for preheating the feedwater and/or steam flow to the HTSE unit. This section presents the approach and major assumptions for evaluating the HTSE-AGR-SCO_2 system configuration utilizing thermal recuperation from the product gases and/or the SCO_2 cycle.

IV.A.1. Approach

For estimating the efficiency of the HTSE-SCO_2-AGR, we obtain a coupled solution of the following tasks:

1. evaluating the electrical energy needed for the electrolysis of steam. For this task, we performed thermodynamic calculations relevant to HTSE reversible and irreversible operation at a given temperature and pressure.
2. obtaining the electricity production efficiency. For this task, we used the thermodynamic analysis code developed by Dostal[10] for the SCO_2 recompression Brayton cycle and modified it to accommodate the changes in the SCO_2 system for a specific design layout for HTSE-SCO_2-AGR.
3. evaluating heat exchanger conditions. For this task, we performed thermodynamic calculations for additional heat exchangers needed in the integrated system for thermal regeneration.
4. matching the H_2 production pressure to the distribution infrastructure pressure. For this task, we evaluated the power required for pumping the water and/or for compressing the hydrogen to the distribution infrastructure pressure. In this work, the hydrogen gas pipeline infrastructure inlet pressure is chosen at a conservative value of 7 MPa.

IV.A.2. Assumptions

Three main assumptions made in the analytical evaluation of improved design layout in this work are related to HTSE system properties, product stream temperature at the outlet of the HTSE unit, and heat exchanger effectiveness in a range of operating conditions.

IV.A.2.a. HTSE Unit Properties.

1. The materials and size of the HTSE unit SOECs' electrodes and electrolyte have not been specified for this

analysis. In Sec. II, we stated that each candidate set of SOEC materials may yield a specific level of performance associated with the magnitude of irreversibilities in the electrochemical process. Here, we adopt a range of fractional electrical energy loss due to irreversibilities in the HTSE process for producing a unit amount of hydrogen. The ideal (minimum) amount of electrical energy needed in the HTSE process is the Gibbs free energy change ΔG for the electrolysis reaction at a given temperature and pressure. Hence, the actual amount of electrical energy needed for the HTSE process, W_{ES}, in this analysis is taken as

$$W_{ES} = \Delta G_{ES} + W_{ES\text{-}OP} \ , \qquad (7)$$

where

$$0.1 \times \Delta G_{ES} \leq W_{ES\text{-}OP} \leq 0.2 \times \Delta G_{ES}$$

ΔG_{ES} = Gibbs free energy change for electrolysis reaction, equivalent to the ideal amount of electrical energy needed for electrolysis

$W_{ES\text{-}OP}$ = electrical energy required to compensate for the overpotentials/irreversibilities in the steam electrolysis cells.

The range taken for the fractional electrical energy losses is based on the performance of the current SOFC technology and expected future development.

2. The inlet flow to the HTSE unit is pure steam at the desired temperature and pressure. Certain SOEC cathode materials can be susceptible to oxidation and degradation when exposed to high-steam partial pressure. For instance, the most conventional SOFC anode Ni-YSZ cermet can serve as the cathode of SOECs. Nevertheless, Ni fine particles in the cermet are subject to oxidation and consequently agglomeration, which deteriorates the electrode performance under a high-steam-concentration environment. The degradation of the Ni-YSZ cathode can be slowed down and stabilized by including hydrogen along with steam at the inlet for the cathode of the SOEC. This approach does not completely solve the electrode performance degradation problem. Moreover, other materials development can potentially serve as better SOEC cathodes, which do not degrade (or degrade minimally) under high steam content, while maintaining high catalytic activity. In such a case, the inlet stream to the HTSE can be taken as pure steam. In this analysis, we assume that the inlet stream is only high-temperature steam, and that the SOEC cathode is chosen to accommodate this condition without significant degradation. Hence, the range of irreversible energy losses described above is likely to be still valid. In terms of thermodynamics, even with excess H_2 at the inlet stream, it would be recycled/regenerated within the plant and would not cause a significant effect on system efficiency. The excess H_2 that enters and exits the HTSE does not affect the energy balance in the HTSE unit, and the preheating and postcooling of the excess H_2 can be balanced in the plant.

3. Water vapor can coexist with hydrogen at the outlet of the HTSE if the HTSE unit is designed such that the inlet steam flow cannot dissociate completely by electrolysis. In this analysis, we assume that the HTSE unit utilizes all the steam to be electrolyzed to produce only hydrogen and oxygen at the outlet. If excess $H_2O_{(g)}$ along with product H_2 were present at the exit of the HTSE unit, the separation of $H_2O_{(g)}$ from the product stream can take place by condensing the steam while recuperating the thermal energy content of the outlet streams of the HTSE unit.

IV.A.2.b. Temperature of Product Gases. The temperature of the product gases (hydrogen and oxygen) at the outlet of the HTSE unit depends on three factors:

1. the inlet steam temperature
2. the rate of heat production in the HTSE unit. The cell irreversibilities, which require additional applied electrical potential on the SOEC cells, convert to heat production in the cells. The heat production can help increase the temperature of the electrolysis process and consequently that of the product gases.
3. the rate of heat loss from the HTSE unit.

Here, we assume that the SOECs are designed to operate at a current density that allows for adiabatic operation of the HTSE unit, with no net heat loss or generation. Thus, the temperature of the outlet product streams can be taken the same as that of the inlet stream.

IV.A.2.c. Heat Exchanger/Recuperator Effectiveness. One of the main goals of this design work is to keep the integrated system as compact as possible, as was the case for the SCO_2 system development. The PCHEs by the British company Heatric are currently the most effective and compact heat exchangers and have been recommended in the development of the SCO_2 cycle for accommodating large pressure differentials.[10] We also choose to use this technology as recuperators for regenerating the heat from the product streams to preheat the water/steam. Thus, we utilize the performance features of the PCHEs in the evaluation of plant efficiency. A major advantage of the Heatric units is their ability to operate at high temperatures and under high pressure. Figure 10 shows the current operating experience of Heatric heat exchangers. Figure 10 and informative communication with Heatric (Ref. 21) indicate that our intended application can fall within the current reliable operating limits of the PCHEs if the highest temperature (the HSTE temperature) and the pressure at the highest temperature location are limited to 900°C and 3 MPa, respectively. Nevertheless, Heatric is developing new materials that can operate well at 900°C but also at higher

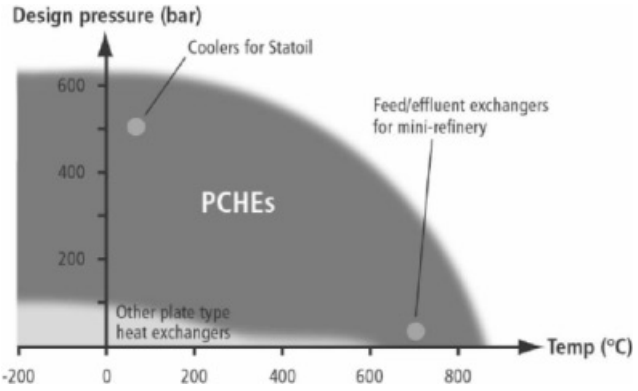

Fig. 10. Current operating experience of Heatric PCHEs (Ref. 20).

pressures, and the materials composition is currently kept confidential. Based on PCHE features, we also assume that the hot side with inlet temperature of $T_{H,in}$ in a recuperator can raise the cold-side outlet temperature up to $T_{C,out} = T_{H,in} - 30°C$.

IV.B. Integrated Plant Component Analysis

In HTSE-SCO_2-AGR in this work, hydrogen is the main product, and the electricity production level is just sufficient for accomplishing the electrolysis and for supporting the plant. The plant can be designed to incorporate a separation distance or a separation barrier between the nuclear reactor and the hydrogen production process for ensuring an acceptable level of safety of the integrated plant. However, the actual form of this separation, if any, and its safety implications are still to be investigated. This work assumes a physical barrier instead of a separation distance to eliminate accident propagation between the nuclear and hydrogen plants. Consequently, the heat losses due to transporting the fluids from the nuclear plant for heating the water/steam at the electrolysis plant are presumed negligible.

IV.B.1. Energy Balance for Plant Components

IV.B.1.a. HTSE Unit. A thermodynamic analysis of the steam electrolysis process is needed for determining the energy efficiency of the integrated plant. The energy needed for dissociation of steam as $H_2O_{(g)} \rightarrow H_{2(g)} + \frac{1}{2}O_{2(g)}$ is

$$\Delta H_{ES} = Q_{th,ES} + \Delta G_{ES} \ , \tag{8}$$

where

$Q_{th,ES}$ = thermal energy (provided by the reactor or by thermal recuperation from product gases or the working fluid of the power conversion system) for preheating water/steam to the electrolysis temperature. In this work, the HTSE unit is taken to operate at a voltage where the endothermic heat of reaction for electrolysis is compensated by the irreversible dissipation of overpotentials as heat in the HTSE unit SOEC cells. Thus, $Q_{th,ES}$ does not include the endothermic heat of reaction.

ΔG_{ES} = Gibbs free energy change for the electrolysis reaction, which corresponds to the ideal (minimum) amount of electrical energy needed for the electrolysis of H_2O at a given temperature and pressure to produce a unit amount of H_2.

The total thermal energy $Q_{th,ES}$ required for preheating the water/steam is evaluated as

$$\begin{aligned} Q_{th,ES} &= Q_{th,Reactor} + Q_{th,Recup} \\ &= \dot{m}_{H_2O}(h_{H_2O,out} - h_{H_2O,in}) \\ &= \dot{m}_{H_2O}\left(\int_{T_{H_2O,in}}^{T_{H_2O,sat}} c_p(T)\,dT + h_{fg} \right. \\ &\qquad \left. + \int_{T_{H_2O,sat}}^{T_{HTSE}} c_p(T)\,dT \right) \ , \end{aligned} \tag{9}$$

where

$Q_{th,Reactor}$ = thermal energy provided directly by the nuclear reactor (or indirectly by the working fluid of the power conversion system) for preheating water/steam to a higher temperature

$Q_{th,Recup}$ = thermal energy provided by thermal recuperation from product gases for preheating water/steam to a higher temperature

$\dot{m}_{H_2O}$ = mass flow rate of feed water/steam in the system

h = enthalpy

c_p = heat capacity, a function of temperature at a given pressure

h_{fg} = heat of vaporization for H_2O at a given pressure

$T_{H_2O,sat}$ = saturation temperature of H_2O at a given pressure

T_{HTSE} = steam electrolysis temperature.

The total thermal energy transfer to water/steam can take place in multiple steps with more than one heat exchanger. This can involve heat transfer from the reactor coolant, the product gases, and the working fluid of

the power conversion system (in a direct cycle plant, the working fluid and the reactor coolant are the same).

$$Q_{th,ES} = \sum_{j=1}^{N} \dot{m}^{j}_{H_2O}(h^{j}_{H_2O,out} - h^{j}_{H_2O,in}) = \sum_{j=1}^{N} \dot{m}^{j}_{HF}(h^{j}_{HF,in} - h^{j}_{HF,out}) \ , \quad (10)$$

where

$\dot{m}_{HF}$ = mass flow rate of feed hot fluid heating the water/steam flow

N = number of heat exchangers for heating the water/steam flow in the plant

j = j'th heat exchanger where $j = 1$ to N.

The actual amount of electrical energy needed for the electrolysis, as explained in Sec. II, should include the overpotential-related electrical energy losses that need to be compensated for, namely, those due to the irreversibilities that arise from activation of the reaction intermediate steps, the mass transfer limitations, and the ohmic resistances. Thus, the actual amount of electrical energy needed for electrolysis to produce a unit amount of H_2 can be expressed as W_{ES}:

$$W_{ES} = E \times n_e \Im = \Delta G_{ES} + W_{ES\text{-}OP} = \Delta G_{ES} + \eta \times n_e \Im \ , \quad (11)$$

where the cell potential is $E = E_r + \eta$. W_{ES} is supplied by the power conversion system that is adopted into the design concept for the plant.

IV.B.1.b. Reactor. The SCO_2 cools the reactor and undergoes enthalpy change equivalent to the total reactor power Q_{th}:

$$Q_{th} = \dot{m}_{CO_2}(h_{CO_2,out} - h_{CO_2,in}) \ . \quad (12)$$

The enthalpy carried by the SCO_2 is converted to electrical energy by the SCO_2 recompression cycle and to the thermal energy of the water/steam by its preheating before the electrolysis unit.

IV.B.1.c. SCO_2 Power Conversion System. The SCO_2 power conversion system is sized to produce enough electricity for supplying the HTSE unit W_{ES} and for supporting the plant in this analysis. The thermal energy required by the power conversion system Q_{th,SCO_2} is equivalent to

$$Q_{th,SCO_2} = \frac{W_{ES}}{\eta_{SCO_2}} + \frac{W_P + W_C}{\eta_{SCO_2}} \ , \quad (13)$$

where

η_{SCO_2} = efficiency of the SCO_2 recompression Brayton cycle

W_P, W_C = work required for pumping or compressing the fluids related to the HTSE process in the plant.

The cycle efficiency values η_{SCO_2} are based on the analysis done by using the thermodynamic analysis code for the SCO_2 cycle given the operating conditions defined for each plant configuration.

IV.B.1.d. Heat Exchangers. For each heat exchanger that is used for heating the feedwater/steam to the HTSE unit, the heat balance is established as follows:

$$\dot{m}^{j}_{H_2O}(h^{j}_{H_2O,out} - h^{j}_{H_2O,in}) = \dot{m}^{j}_{HF}(h^{j}_{HF,in} - h^{j}_{HF,out}) \ . \quad (14a)$$

We apply a condition on regeneration in the recuperating heat exchangers that the hot side with inlet temperature of $T_{H,in}$ in a recuperator can raise the cold-side outlet temperature up to $T_{C,out} = T_{H,in} - 30°C$.

The electrical heating that can be necessary for raising the steam temperature at the inlet of the HTSE unit to the process temperature is considered similarly and is found as

$$Q_{elec\text{-}heating} = \frac{W_{elec\text{-}heating}}{\eta_{SCO_2}} = \frac{\dot{m}^{j}_{H_2O}(h^{j}_{H_2O,out} - h^{j}_{H_2O,in})}{\eta_{SCO_2}} \ . \quad (14b)$$

Equations (7) through (14) are solved as a set of coupled thermal energy balance to find the state of the feedwater/steam and the energy transfer at each step for each configuration that is evaluated.

IV.B.1.e. Pumping and Compression. The product hydrogen should be delivered at a pressure that matches the distribution infrastructure pressure. This can be achieved in three ways:

1. electrolyzing steam at atmospheric pressure and compressing the product hydrogen gas up to the distribution infrastructure pressure
2. pumping water up to the distribution infrastructure pressure and electrolyzing steam at this high pressure
3. partially pumping water to be electrolyzed at relatively high pressure and by additional compression of the product hydrogen to match the distribution infrastructure pressure.

All three cases are evaluated in this work for different plant configurations.

The work required for pumping the water to the desired pressure is evaluated as

$$W_P = \frac{W_{P,ideal}}{\eta_P} = \frac{\dot{m}_{H_2O}(h_{P,out,s} - h_{P,in})}{\eta_P} \quad , \qquad (15)$$

where

$W_{P,ideal}$ = ideal (minimum) work spent for pumping a fluid up to a higher pressure

η_P = pump efficiency (0.85 in this work)

$h_{P,out,s}$ = ideal enthalpy of the fluid at the exit of the pump after isentropic compression.

The work required for compressing the hydrogen produced at the HTSE system pressure to the desired distribution pressure is evaluated as

$$W_C = \frac{W_{C,ideal}}{\eta_C} = \frac{\dot{m}_{H_2}(h_{C,out,s} - h_{C,in})}{\eta_C}$$

$$= \frac{1}{\eta_C}\dot{m}_{H_2} RT_{in}\left(\frac{k}{k-1}\right)\left(\left(\frac{P_{H_2,out}}{P_{H_2,in}}\right)^{(k-1)/k} - 1\right) \quad ,$$

where

$$k = c_p/c_v \qquad (16)$$

$W_{C,ideal}$ = ideal (minimum) work spent for pumping a fluid up to a higher pressure

η_C = compressor efficiency (0.85 in this work)

$\dot{m}_{H_2}$ = mass flow rate of hydrogen.

IV.B.2. Hydrogen Production Efficiency

The energy efficiency of the hydrogen production using the HTSE process, $\eta_{H,p}$, is estimated as the ratio of the heating value of hydrogen to the total thermal energy needed to drive the electrolysis process:

$$\eta_{H,p} = \frac{\Delta H_{r,H_2}}{Q_{th,ES,Reactor} + \dfrac{\Delta G_{ES} + W_{ES\text{-}OP}}{\eta_{SCO_2}}} \quad . \qquad (17)$$

The hydrogen production process efficiency $\eta_{H,p}$ for different processes has usually been the means of comparison among different hydrogen production alternatives. The overall thermal-to-hydrogen energy conversion efficiency of the nuclear hydrogen production plant for each configuration is then calculated as

$$\eta_H = \frac{\Delta H_{r,H_2}}{Q_{th,ES,Reactor} + \dfrac{(\Delta G_{ES} + W_{ES\text{-}OP}) + W_P + W_C}{\eta_{SCO_2}}} \quad , \qquad (18)$$

where

$\Delta H_{r,H_2}$ = enthalpy of reaction for the combustion of $H_{2(g)}$ with oxygen, equivalent to the heating value of hydrogen, which is the energy that can be recovered by oxidizing $H_{2(g)}$. Low heating value of hydrogen (LHV_H) is used for evaluating the hydrogen production process efficiency in this work.

$W_{ES\text{-}OP}$ = electrical energy required to compensate for the overpotentials/irreversibilities in the steam electrolysis cells. The dissipation of overpotential work term as heat in the SOECs is not taken explicitly here. This is due to the assumption that the operating voltage is chosen such that the irreversible heat generation term compensates for the endothermic heat of electrolysis reaction in the SOECs.

IV.C. Plant Layout Evaluation

The integration of the nuclear and hydrogen plants should incorporate thermal energy recuperation (regeneration) as much as feasible. The purpose of the regeneration of thermal energy is to preheat the feedwater/steam before it reaches the HTSE unit, thus reducing the required reactor power. Multiple stages of regeneration can be incorporated on the path of the feedwater/steam to improve the efficiency of the plant. Nevertheless, each stage of thermal regeneration involves an additional heat exchanger/recuperator that increases the capital cost of the plant. A compromise is to be achieved between the additional recuperators and the increase in the capital cost of the proposed design.

The high-temperature product gases from the HTSE unit are the obvious hot flow streams from which to recuperate heat. They leave the HTSE unit at the electrolysis temperature T_{ES} with significant thermal energy content. Therefore, they can be used for preheating the steam at high temperatures. With sufficiently high HTSE temperature, the product gases can be at temperatures greater than that of the reactor exit $T_{R,out}$. This configuration can give the flexibility for removing the burden of attaining very high temperature at the reactor exit as for the reactors proposed for driving high-temperature thermochemical water-splitting processes. For the purpose of this work, the electrolysis temperature is taken as 900°C, and possible arrangements have been evaluated for improving the integration of the systems to provide the

900°C of steam to the HTSE unit in the most efficient way. The proposed scheme is presented here.

IV.C.1. Recuperative HTSE-AGR-SCO_2: Intermediate Temperature and Intermediate Pressure IHX

Figure 11 shows the flow diagram for the HTSE-AGR-SCO_2 integrated plant configuration in this work, using thermal regeneration from the hydrogen and oxygen product streams by two separate recuperators, R_O and R_H. The preheating of water is accomplished through an intermediate heat exchanger (IHX) between the SCO_2 turbine exit and the feedwater streams. An electrical heater provides heat to raise the temperature of the feed steam to the electrolysis temperature to compensate for the inefficiency of the recuperators R_O and R_H.

The IHX in the configuration shown in Fig. 11 could also be placed at the flow stream from the exit of AGR. In that case, the IHX would be subject to higher pressure differential between the hot and cold sides and at relatively high temperature at the inlet of the hot side. The hot-side pressure in IHX would be ~20 MPa, and the inlet temperature would range from 550 to 700°C depending on the design option. The cold-side pressure could range from atmospheric to 7 MPa, and the inlet temperature would be ambient (30°C). A more feasible configuration involves heat transfer by recuperation from a relatively lower temperature and pressure flow stream in the plant. Reducing the thermal and pressure gradients in the IHX provides better flexibility in choosing durable but less costly structural materials for the IHX. The alternative to preheat and boil the feedwater should not significantly interfere with the simplicity of the SCO_2 cycle while still having enough heat capacity to bring the feedwater to saturated steam condition at the pressure of the cold side of the IHX. The best candidate stream for this process is the exit from the SCO_2 turbine as represented in Fig. 11, instead of the high-pressure high-temperature exit from the AGR.

IV.C.2. Advantages of the Recuperative HTSE-AGR-SCO_2 with Intermediate Temperature and Intermediate Pressure IHX

In addition to the expected gain in IHX cost and durability due to less harsh thermal and pressure gradients, there are two more advantages for the configuration in Fig. 11 over that with the IHX at the AGR exit. The first is the flexibility that can be brought to controlling the electricity and hydrogen production rates with respect to each other in a limited range. It is very likely that a utility may prefer to adjust the electrical output depending on demand, while keeping the reactor power the same, in order to maximize profits. Hydrogen can be stored at low peak hours, and the demand for hydrogen can be followed by the help of onsite storage units. However, electricity demand cannot be followed in the same manner. The configuration in Fig. 11 can accomplish regulation of the electricity production rate closer to the electricity demand only by adjusting the feedwater flow rate sent to the IHX.

The hydrogen and oxygen product streams have high heat capacity, however, they are not sufficient to raise the temperature of the feedwater from ambient to above

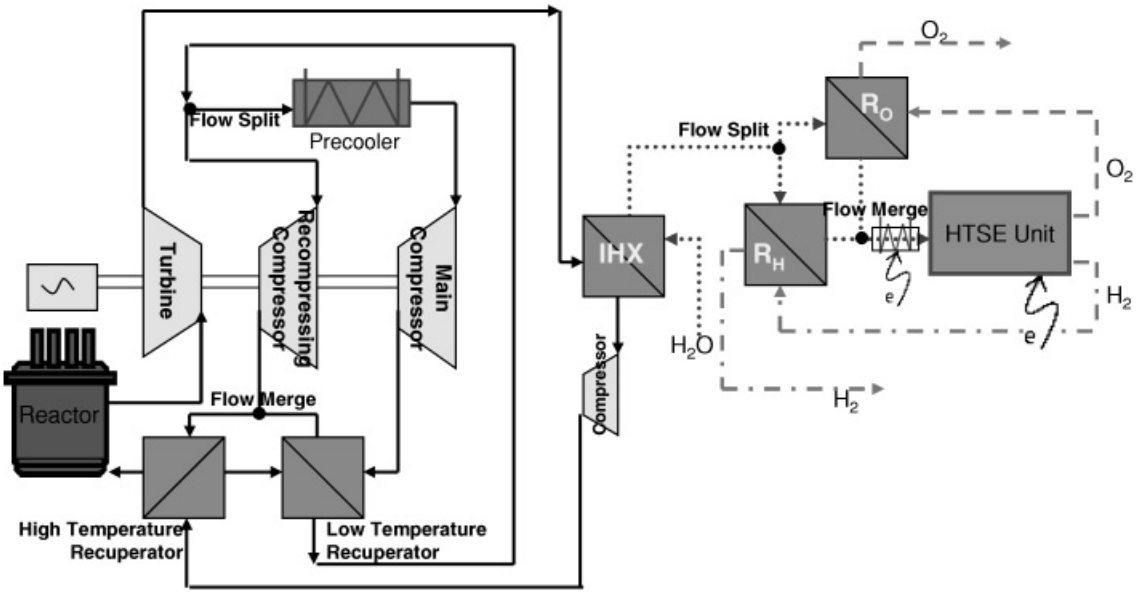

Fig. 11. Schematic showing the integrated HTSE-SCO_2-AGR plant, with recuperation of heat into steam from hydrogen and oxygen flow streams and with heat provided from the SCO_2 turbine exit for boiling the feedwater stream.

boiling. The total energy needed for raising the temperature of water up to 900°C is decomposed as below:

$$Q_{th,ES} = \dot{m}_{H_2O}\left(\int_{T_{H_2O,in}}^{T_{H_2O,sat}} c_p(T)\,dT + h_{fg} + \int_{T_{H_2O,sat}}^{T_{HTSE}} c_p(T)\,dT \right) . \quad (19)$$

Specifically, the heat of vaporization, h_{fg}, amounts to the highest fraction of energy requirement. The thermal energy that can be transferred to the feedwater is less than this value. Therefore, boiling of the feedwater should at least be started by heat transfer from the IHX with the SCO_2 as the heat source. For the feasibility of the configuration, we decide to have the boiling of the feedwater start and complete only at one location/component in the system. Hence, the IHX serves as a boiler for the feedwater, and the feedwater exits the IHX as saturated steam for a given pressure, $T_{H_2O,sat}$. The rest of the heat transfer required for raising the steam temperature to T_{ES} (= 900°C) is taken from the hydrogen and oxygen product streams in R_H and R_O and from the electrical heater. Since, the recuperators in the system are assumed to be of the PCHE type, the steam can be raised to a temperature 30°C below the products' highest temperature (that is also the HTSE temperature). Hence, the electrical heater supplies heat for raising the temperature of steam from 870 to 900°C at a given pressure.

If the feedwater flow rate into the IHX decreases, the temperature of the hot-stream CO_2 at the exit of the IHX that goes into the high-temperature recuperator increases. The increase in the temperature of this stream causes an increase in the reactor inlet temperature. With a constant nuclear power, the temperature of the SCO_2 coolant at the reactor increases. Consequently, the efficiency of the electricity production system increases, and more electricity is produced. At the same time, the rate of hydrogen production decreases because of the lower feedwater flow rate. The opposite sequence will occur if the feedwater flow rate to the IHX is increased.

The second main advantage is the additional separation of the hydrogen production process from the nuclear reactor by means of coupling the HTSE unit to the SCO_2 cycle rather than the reactor. In this way, the flow stream of the hydrogen is farther away from a flow stream that is directly coupled to the reactor. This can yield better safety implications.

IV.C.3. Performance of the Recuperative HTSE-AGR-SCO_2

Evaluation of the plant efficiency for the configuration in Fig. 11 considers electricity production only sufficient to drive hydrogen production. The unit amount of hydrogen production rate is taken as 1 kg/s. The base case pressure for the HTSE unit is taken as 1 atm. The base design for the recuperative configuration of the HTSE-SCO_2-AGR assumes a conservative performance of the turbomachinery in the SCO_2 cycle. Table IV summarizes the results for the electricity and hydrogen production efficiency, reactor inlet temperature, and the ratio of flow rates of CO_2 and H_2. The fractional reactor power needed for the preheating and boiling of the feedwater is presented for the base case pressure at two temperatures for the reactor exit: 550 and 650°C.

The results in Table IV, compared to those in Table III, indicate that, at the base case pressure operation, the recuperative configuration improved the efficiency of the process by 16% fractional (6.5% absolute) and 13% fractional (6% absolute) for reactor exit temperatures of 550 and 650°C, respectively. In this comparison, neither the nonrecuperative nor the recuperative configurations include the compression of the product hydrogen for delivery.

TABLE IV

The Results for the Base Case Recuperative HTSE-SCO_2-AGR Configuration Represented in Fig. 9 with Conservative Turbomachinery Design in SCO_2 Cycle

Electrolysis pressure (MPa); temperature (°C)	0.1; 900					
Reactor exit temperature, $T_{R,out}$ (°C)	550			650		
Design based on turbomachinery efficiency	Conservative			Conservative		
Reversible cell voltage, E_r (V)	−0.933			−0.933		
Overpotential (% of E_r)	0	10	20	0	10	20
Percent of reactor power for H_2O preheating, R (%)	10.0	9.2	8.5	10.7	9.9	9.1
Reactor inlet temperature, $T_{R,in}$ (°C)	386.2	387.6	388.8	470.3	471.9	473.4
Ratio of flow rates (m_{CO_2}/m_{H_2})	1237	1357	1520	1020	1112	1220
Electrical efficiency, η_{el} (%)	39.1	39.5	39.7	42.0	42.4	42.7
Process hydrogen efficiency, $\eta_{H,p}$ (LHV, %)	51.8	47.5	43.9	55.6	51.0	47.2

IV.C.4. Effect of HTSE Pressure on the Performance

It is easier to distribute the product gas to the pipelines at significantly higher pressures than atmospheric pressure. This can be achieved in three ways: compressing the hydrogen produced at atmospheric pressure up to the distribution pressure, pumping the feedwater to the required high pressure prior to when the HTSE takes place, or a combination of both schemes. The high-pressure production of hydrogen at HTSE saves compression energy since the work needed for pumping the water up to the required high pressure [W_P in Eq. (15)] is less than that required for compressing the product hydrogen from atmospheric pressure at high temperature to the same high pressure [W_C in Eq. (16)]. A constraint on the limit of the pressure that HTSE can operate is the capability of the recuperator (R_O and R_H) materials to handle the 900°C hot-side temperature reliably at high pressures. As seen in Fig. 10, the currently reliable operating experience of PCHE-type recuperators is within 3 MPa at a maximum temperature of 900°C. Meanwhile, communication with Heatric representatives indicates that PCHE materials stronger than the current materials will be available in the near future. On the other hand, the electrical energy required in the HTSE unit increases at high pressure since the change in Gibbs free energy of the reaction increases with pressure. The increase in the HTSE energy requirement can balance or overcome the energy savings from compression. Another advantage of high-pressure operation in the HTSE unit is the expected significant reduction in the size of the HTSE components and units that consequently can reduce their capital cost of the HTSE unit. However, the walls and the leak-tightness of the components will be more expensive. Hence, the optimal operating high pressure can be a compromise between the gain from H_2-compression work, loss from electrical energy needed for the HTSE process, and the net gain or loss from the capital cost of the recuperative HSTE unit. We do not evaluate the economics of this configuration in this paper and consider the high-pressure operation of the recuperative HTSE-SCO_2-AGR within a pressure range of 3 to 7 MPa for its effect on the efficiency.

Figure 12 and Tables V and VI show the temperature of flow streams and flow ratios at different locations of the HTSE recuperative unit. The flow-split ratio into streams 2a and 2b for $H_2O_{(g)}$ is found such that the temperatures at 3a and 3b are equal ($T_{3a} = T_{3b}$) and temperatures at 6 and 8 are equal ($T_6 = T_8$). Even if they were not taken equal, the flow split would be adjusted to satisfy the energy balance. Another criterion for the stated temperatures would yield the same energy efficiency values as long as $H_2O_{(g)}$ is raised to the same temperature (30°C below the HTSE temperature) starting from saturated steam condition using only the H_2 and O_2 product gas streams.

It can be seen from Table VII and Fig. 13 that as the pressure of the high-temperature electrolysis increases, the efficiency of producing hydrogen (without/before compression), $\eta_{H,P}$, with this process decreases. This is due to the increasing Gibbs free energy change of the electrolysis reaction with increasing pressure. The evaluation is based on a system where the feedwater range of pressures (0.1 to 7 MPa in this case) is available to the system starting from the inlet of the IHX. Thus, the work

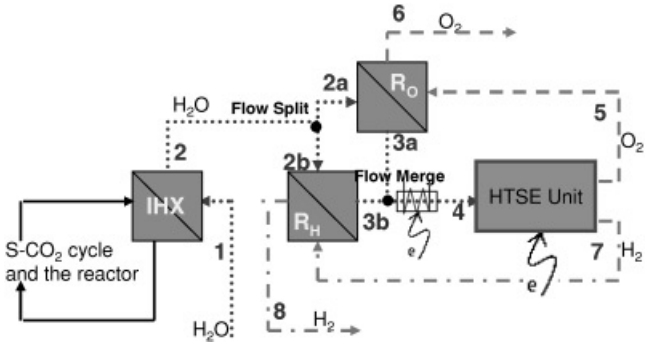

Fig. 12. Schematics of recuperation and HTSE unit within the HTSE-SCO_2-AGR.

TABLE V

Temperature of Flow Streams (H_2O, H_2, and O_2) at Different Locations

Point	P = 0.1 MPa Temperature (°C)	P = 3 MPa Temperature (°C)	P = 7 MPa Temperature (°C)
1	30.0	30.0	30.0
2	100.0	233.9	278.2
2a	100.0	233.9	278.2
2b	100.0	233.9	278.2
3a	870.0	870.0	870.0
3b	870.0	870.0	870.0
4	900.0	900.0	900.0
5	900.0	900.0	900.0
6	265.8	345.7	346.0
7	900.0	900.0	900.0
8	265.8	345.7	346.2

TABLE VI

Flow Split Ratios of H_2O Before Recuperators

Percent of Flow in	P = 0.1 MPa	P = 3 MPa	P = 7 MPa
Stream a	36.3	36.5	36.6
Stream b	63.7	63.5	63.4

TABLE VII

Comparison of the Process and Overall Energy Efficiency for the Recuperative HTSE-SCO_2-AGR Plant Configuration Represented in Figs. 11, 12, and 14 Under Different Operating Conditions

Electrolysis pressure (MPa); temperature (°C)	0.1; 900					
Reactor exit temperature, $T_{R,out}$ (°C)	550			650		
Design based on turbomachinery efficiency	Conservative			Conservative		
Overpotential (% of E_r)	0	10	20	0	10	20
Process hydrogen efficiency, $\eta_{H,p}$ (LHV, %)	51.8	47.5	43.9	55.6	51.0	47.2
Overall hydrogen efficiency, η_H (LHV, %)	47.0	43.5	40.4	49.6	45.9	42.8
Electrolysis pressure (MPa); temperature (°C)	3; 900					
Reactor exit temperature, $T_{R,out}$ (°C)	550					
Design based on turbomachinery efficiency	Conservative			Best Estimate		
Overpotential (% of E_r)	0	10	20	0	10	20
Process hydrogen efficiency, $\eta_{H,p}$ (LHV, %)	47.7	43.8	40.5	49.6	45.3	41.9
Overall hydrogen efficiency, η_H (LHV, %)	46.1	42.4	39.3	47.8	43.8	40.6
Electrolysis pressure (MPa); temperature (°C)	7; 900					
Reactor exit temperature, $T_{R,out}$ (°C)	550					
Design based on turbomachinery efficiency	Conservative			Best Estimate		
Overpotential (% of E_r)	0	10	20	0	10	20
Process hydrogen efficiency, $\eta_{H,p}$ (LHV, %)	46.8	42.9	39.7	48.7	44.8	41.4
Overall hydrogen efficiency, η_H (LHV, %)	45.2	41.6	38.6	47.0	43.3	40.2
Electrolysis pressure (MPa); temperature (°C)	3; 900					
Reactor exit temperature, $T_{R,out}$ (°C)	650					
Design based on turbomachinery efficiency	Conservative			Best Estimate		
Overpotential (% of E_r)	0	10	20	0	10	20
Process hydrogen efficiency, $\eta_{H,p}$ (LHV, %)	51.1	46.7	43.4	52.5	48.7	44.8
Overall hydrogen efficiency, η_H (LHV, %)	49.2	45.1	42.0	50.4	46.9	43.3
Electrolysis pressure (MPa); temperature (°C)	7; 900					
Reactor exit temperature, $T_{R,out}$ (°C)	650					
Design based on turbomachinery efficiency	Conservative			Best Estimate		
Overpotential (% of E_r)	0	10	20	0	10	20
Process hydrogen efficiency, $\eta_{H,p}$ (LHV, %)	50.3	46.1	42.6	52.1	47.7	44.3
Overall hydrogen efficiency, η_H (LHV, %)	48.5	44.6	41.3	50.1	46.1	42.9
Electrolysis pressure (MPa); temperature (°C)	3; 900					
Reactor exit temperature, $T_{R,out}$ (°C)	700					
Design based on turbomachinery efficiency	Conservative			Best Estimate		
Overpotential (% of E_r)	0	10	20	0	10	20
Process hydrogen efficiency, $\eta_{H,p}$ (LHV, %)	52.50	48.20	44.80	54.40	50.10	46.20
Overall hydrogen efficiency, η_H (LHV, %)	50.4	46.4	43.3	52.2	48.2	44.6
Electrolysis pressure (MPa); temperature (°C)	7; 900					
Reactor exit temperature, $T_{R,out}$ (°C)	700					
Design based on turbomachinery efficiency	Conservative			Best Estimate		
Overpotential (% of E_r)	0	10	20	0	10	20
Process hydrogen efficiency, $\eta_{H,p}$ (LHV, %)	51.60	47.70	43.80	53.50	49.10	45.30
Overall hydrogen efficiency, η_H (LHV, %)	49.7	46.1	42.4	51.4	47.4	43.8

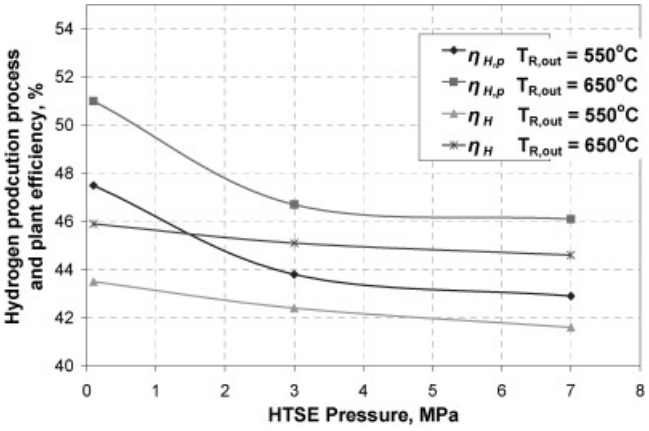

Fig. 13. Comparison of the process ($\eta_{H,P}$) and overall energy efficiency (η_H) for the recuperative HTSE-SCO_2 AGR plant configuration represented in Figs. 11 and 14 for different reactor exit temperatures with HTSE operating at 90% voltage efficiency.

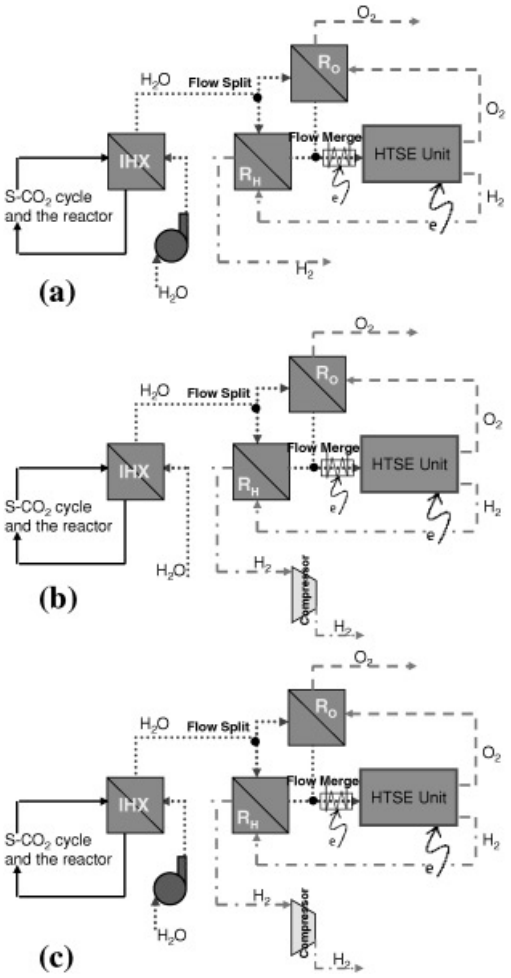

Fig. 14. Schemes for raising the pressure of the product hydrogen up to 7 MPa: (a) pumping the feedwater up to 7 MPa for HTSE and distribution at 7 MPa; (b) compressing the H_2 produced at 1 atm up to 7 MPa; and (c) pumping the feedwater to 3 MPa and the H_2 produced at 3 MPa up to 7 MPa.

needed for pumping the feedwater to a required pressure is not included. In addition, the supplementary compression of the produced hydrogen up to the distribution infrastructure pressure (7 MPa in this case) is not considered within $\eta_{H,P}$. Figure 14 shows configurations where the product H_2 can be brought up to the distribution pressure. The layout in Fig. 14a includes additional pumping to raise the pressure of feedwater to the required distribution pressure at which the HTSE unit operates. The layout in Fig. 14b considers additional compression of H_2 produced at 1 atm up to the distribution pressure. The layout in Fig. 14c considers pumping the feedwater to an intermediate pressure (3 MPa in this case) and further compressing the H_2 produced at the intermediate pressure up to the distribution pressure.

Table VII and Fig. 13 also present the comparison of the overall hydrogen production efficiency η_H of the integrated recuperative HTSE-SCO_2-AGR plant as shown in Figs. 11, 12, and 14. The overall plant hydrogen production efficiency η_H includes the work spent for pumping and compression in different pressurization schemes. An optimal pressure cannot be chosen based only on the plant efficiency values. The overall plant hydrogen production efficiency η_H decreases with increasing pressure (in a less sharp way than the decrease for the process efficiency $\eta_{H,P}$). An improvement in capital cost and feasibility is expected from downsizing of the HTSE unit at relatively high pressures. A similar advantageous overall effect of pressure is expected for the cost of the gas-cooled reactors, as discussed by Schlenker.[22] However, a coupled cost and efficiency analysis is required to find out the quantitative implications of HTSE operating pressure on economics and to decide on the optimal operating pressure. The coupled effect of system pressure on efficiency, capital cost, and product cost can be qualitatively shown as in Fig. 15. We expect that an intermediate pressure can be preferential.

IV.C.5. Additional Low-Temperature Recuperation from the Product Gases

The exit temperatures of the product gases after the high-temperature recuperators R_O and R_H are significantly high, as seen in Table V, especially at higher pressures. Alternatives for utilizing the thermal energy content of the product gases after the high-temperature recuperators R_O and R_H are discussed in this section as follows.

1. *Produce steam for driving a Rankine cycle to generate additional electricity:* At 7 MPa, the stochiometrically produced 1 kg of H_2 and 8 kg of O_2 can heat

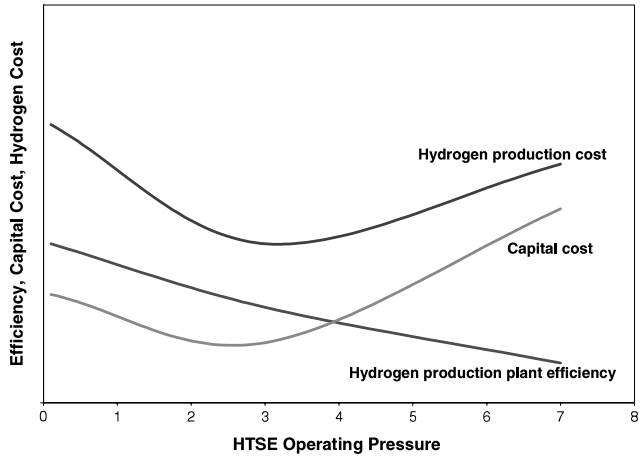

Fig. 15. Effect of HTSE pressure on plant efficiency, capital cost, and hydrogen production cost. (The plots are not to scale, and show only the qualitative relative behavior.)

2.41 kg of H_2O from 20 to 278°C saturated-steam condition at 7 MPa. In this process, the product gases are assumed to cool from 354 to 60°C, transferring 6.52 MJ heat to make steam. If the steam is sent to a Rankine cycle of 33% efficiency, 2.2 MJ of electrical energy can be produced. The heating value of H_2 is 120 MJ/kg. Thus, for 120-MW(hydrogen) production, an additional 2.2 MW(electric) can be produced. Equivalently, for a 600-MW(hydrogen) capacity plant, an additional 10.8 MW(electric) can be generated. However, the steam cycles are costly, and the amount of additional electricity generation in this case is too small to bring the cost of the product further down. Hence, we do not expect this approach to be economically feasible.

2. *Preheat the feedwater before the boiler (IHX) to saturated liquid-water condition at a given pressure with two additional low-temperature recuperators for the product gases:* The configuration can include further thermal regeneration from the product gases at lower temperatures for preheating the feedwater to the IHX. At 7 MPa for both the product gases and the feedwater side, the low-temperature thermal regeneration can gain 10.7 MJ for a 1-kg hydrogen product. This configuration can improve the plant efficiency by 1.4 to 2%. The cost increase due to the additional heat exchangers should be justified for such a configuration. For nuclear applications Heatric estimates the price of a standard product in stainless steel to be ~$30/kg. If coolant conditions exclude the use of stainless steel, the PCHEs may be manufactured from titanium, which would inflate the price to $120/kg. Heatric PCHEs have an advantageous mass-to-duty ration in tonnes per megawatt of 0.2. For a 600-MW(hydrogen) plant size, 53.5 MW(thermal) would be gained by the low-temperature recuperators. For these conditions, the additional heat exchangers can increase the plant cost by $8.025 million based on the standard product price. For an optimistic cost estimate of $2000 per kilowatt(hydrogen) for a 600-MW(hydrogen) plant as in the configuration of Fig. 11, the gain from efficiency would almost be cancelled out by the additional heat exchangers' cost: The net effect would be a 1.3% decrease in the cost of hydrogen. If the heat exchangers' price or the capital cost of the plant is higher, the net effect on cost can quickly become net increase in cost of product hydrogen. Hence, the configuration including the low-temperature preheating of feedwater before the IHX with the product streams is an option to increase the efficiency further but not a clear justification for an overall benefit on economics.

3. *Improving the thermal recuperation in the SCO_2 cycle:* One of the advantages of the SCO_2 cycle is its simple and compact layout. Hence, bringing H_2 or O_2 to recuperate their heat into the SCO_2 cycle may complicate its simplicity appeal. Moreover, at least the H_2 stream should be kept away from flow streams that are closely coupled to the nuclear reactor for safety purposes.

4. *Process heating:* The thermal energy of the product gases can be used for regional process heating if needed, for instance, for desalination. That depends on the plant proximity to industrial activities and the cost of the connections.

V. CONCLUDING REMARKS AND FUTURE RESEARCH AND DEVELOPMENT REQUIREMENTS

As an alternative for hydrogen production, the HTSE-SCO_2-AGR has advantageous characteristics over other nuclear hydrogen production technologies: a high efficiency of hydrogen production with intermediate reactor exit temperatures. This study indicates that a recuperative design of the HTSE-SCO_2-AGR can have a significantly higher efficiency than the simple layout configuration. The improved recuperative HTSE-SCO_2-AGR has the potential to emphasize the expected energy efficiency and cost advantages of nuclear hydrogen technology over the other alternatives for large-scale hydrogen production. The configuration evaluated in this study indicates that potentially 42.9 to 50.1% (LHV) hydrogen production efficiency is attainable with an HTSE pressure range of 3 to 7 MPa, HTSE temperature of 900°C, HTSE overpotential of 10% of ideal potential, and a reactor exit temperature range of 550 to 700°C. The overall plant efficiency for hydrogen production (including the feedwater pumping and/or hydrogen compression) under the same conditions is 41.6 to 48.2%. The stated efficiency with the reactor exit temperature range is notably higher than that attainable for high-temperature sulfur processes for hydrogen production, as shown in Fig. 3.

In addition to the high efficiency, extensive experience from the commercial AGRs, compactness of the SCO_2 power conversion system, and progress in the SOFC materials field can help the economical development of a future recuperative HTSE-SCO_2-AGR. Thus, the HTSE-SCO_2-AGR development is a logical next step in development of nuclear hydrogen production technologies. As with all new technology concepts, there are research and development requirements and advances needed with the recuperative HTSE-SCO_2-AGR. We identify some of the major needs for HTSE-SCO_2-AGR as follows:

1. *HTSE Materials:* The electrode and electrolyte materials composition and microstructure should be identified specifically to address the improvement of electrochemical performance and durability for solid oxide electrolysis cells. Currently, the most common SOFC materials allow operation above 850°C for good electrochemical performance. The same materials have been tested in laboratory for SOEC operation by several groups, and their feasibility has been shown. Enhanced durability of the HTSE materials and favorable economics are achievable and are more likely with lower-temperature operation of SOECs. Thus, compatible materials for the SOECs' intermediate temperatures of 650 to 750°C should be investigated. It is essential to conduct studies to identify the reaction mechanisms that control the performance of SOECs at molecular level. Only by this understanding can appropriate catalysis materials be developed for SOECs as well as for SOFCs.

2. *AGR Materials:* Durable structural and fuel materials for an SCO_2 coolant environment can be a challenge for the HTSE-SCO_2-AGR. There is extensive experience from commercial AGRs concerning the material issues in CO_2 coolant at ~4 MPa and the proposed solutions based on a combination of materials choice and operational conditions. This experience is very useful in redesigning the AGR to operate at higher pressures. However, fundamental research is needed to confirm that graphite and steel degradation in supercritical pressure CO_2 can be avoided as well or inhibited by using similar solution schemes or by developing more advanced materials.

3. *SCO_2-Cooled AGR Thermal Hydraulics:* Experiments and modeling are needed for determining the physical changes in the properties of the SCO_2. This understanding can help develop schemes to best utilize the heat transfer characteristics of SCO_2 for ensuring safe and effective cooling of a new reactor core design in steady-state operation and transient situations.

4. *System Design:* Detailed systems and component designs with supporting experimental work must be developed to understand the trade-offs between a range of operating conditions, various design configurations, efficiency, safety, and economics. This work has addressed the thermodynamic implications of various operation configurations on efficiency from a promising design layout. A thorough analysis of the design of each major component and the overall interaction and its impact on safety and economics is needed for coupling to the thermodynamic analysis.

The energy efficiency of the recuperative HTSE-SCO_2-AGR as analyzed in this work is more promising over the other leading nuclear hydrogen production technologies, which are the SI and WSP cycles as high-temperature thermochemical processes. In addition, its operation in a less harsh environment can make the HTSE technology more feasible[3] than its high-temperature thermochemical counterparts for hydrogen production. In the near term, the objective must be to expand the research on this promising technology as summarized above in order to have a system available for large-scale hydrogen production with confidence and economy.

REFERENCES

1. B. YILDIZ and M. S. KAZIMI, "Nuclear Energy Options for Hydrogen and Hydrogen-Based Liquid Fuels Production," MIT-NES-TR-001, Massachusetts Institute of Technology (2003).

2. B. YILDIZ and M. S. KAZIMI, "Nuclear Energy Technologies for Hydrogen Production," *Proc. Int. Conf. Advances in Nuclear Power Plants (ICAPP 2004)*, Pittsburgh, Pennsylvania (2004).

3. B. YILDIZ and M. S. KAZIMI "Efficiency of Hydrogen Production Systems Using Alternative Nuclear Energy Technologies," *Int. J. Hydrogen Energy*, **31**, *1*, 77 (2005).

4. "Hydrogen as an Energy Carrier and its Production by Nuclear Power," TECDOC-1085, International Atomic Energy Agency (1999).

5. W. DOENITZ, G. DIETRICH, E. ERDLE, and R. STREICHER, "Electrochemical High Temperature Technology for Hydrogen Production or Direct Electricity Generation," *Int. J. Hydrogen Energy*, **13**, *5*, 283 (1988).

6. R. HINO, H. AITA, K. SEKITA, K. HAGA, and T. IWATA, "Study on Hydrogen Production by High Temperature Electrolysis of Steam," Report 97-064, Japan Atomic Energy Research Institute (1997).

7. C. STOOTS, J. E. O'BRIEN, J. S., HERRING, and P. A. LESSING, "Hydrogen Production from Nuclear Energy via High Temperature Electrolysis," *Proc. Int. Conf. Advances in Nuclear Power Plants (ICAPP 2004)*, Pittsburgh, Pennsylvania (2004).

8. L. E. BRECHER, S. SPEWOCK, and C. J. WARDE, "The Westinghouse Sulfur Cycle for the Thermochemical Decomposition of Water," *Int. J. Hydrogen Energy*, **2**, 7 (1977).

9. L. C. BROWN, G. E. BESENBRUCH, R. D. LENTSCH, K. R. SCHULTZ, J. F. FUNK, P. S. PICKARD, A. C. MARSHALL, and S. K. SHOWALTER, "High Efficiency Generation of Hydrogen Fuels Using Nuclear Power," DE-FG03-99SF21888, U.S. Department of Energy (2003).

10. V. DOSTAL, M. J. DRISCOLL, and P. HEJZLAR, "A Supercritical Carbon Dioxide Cycle for Next Generation Nuclear Reactors," MIT-ANP-TR-100, Massachusetts Institute of Technology (2004).

11. http://www.iwe.uni-karlsruhe.de/english/sofc.php (Apr. 2004).

12. B. YILDIZ, K. HOHNHOLT, and M. S. KAZIMI, "H_2 Production Using High Temperature Steam Electrolysis Supported by Advanced Gas Reactors with Supercritical CO_2 Cycles," MIT-NES-TR-002, Massachusetts Institute of Technology (2004).

13. D. MYERS, J. MAWDSLEY, and B. YILDIZ, "High-Temperature Steam Electrolyzer Materials Development," Final Progress Report FY'05, Argonne National Laboratory (2005).

14. http://www.npp.hu/mukodes/tipusok/gr-e.htm (May 2004).

15. D. A. PASK and R. W. HALL, "Review of the Commissioning and Operational Experience of the Hinkley Point B AGR After Three Years' Power Operation," *Nucl. Energy*, **18**, *4*, 237 (1979).

16. K. H. DENT, "Where Next, AGR?" *Nucl. Energy*, **18**, *4*, 261 (1979).

17. R. W. HALL and C. A. CHAFFEY, "Review of the Operational Experience on the Hinkley Point B AGR over the Past Two Years," *Nucl. Energy*, **21**, *1*, 41 (1982).

18. L. B. FISHKIN, "Prestressed Cast Iron Vessel (PCIV) Use for GEN-IV GFR Applications," MIT-GFR-006, Massachusetts Institute of Technology (2004).

19. "Generation IV Roadmap R&D Scope Report for Gas-Cooled Reactor Systems," Nuclear Energy Research Advisory Committee and the Generation IV International Forum (2002).

20. S. J. DEWSON and C. GRADY, "HEATRIC Workshop at MIT," Massachusetts Institute of Technology (2003).

21. S. J. DEWSON, Heatric, Personal Communication (2004).

22. H. V. SCHLENKER, "Cost Functions for HTR-Direct-Cycle Components," *Atomkernenergie*, **22**, *4*, 226 (1974).